NATIONAL ADVISORY COMMITTEE FOR AERONAUTICS

REPORT No. 353

AIRFOIL PRESSURE DISTRIBUTION INVESTIGATION IN THE VARIABLE DENSITY WIND TUNNEL

By EASTMAN N. JACOBS, JOHN STACK
and ROBERT M. PINKERTON

For sale by the Superintendent of Documents, Washington, D. C. - - - - - - - - - - - - - - - - Price 00 cents

AERONAUTICAL SYMBOLS

1. FUNDAMENTAL AND DERIVED UNITS

	Symbol	Metric		English	
		Unit	Symbol	Unit	Symbol
Length	l	meter	m	foot (or mile)	ft. (or mi.)
Time	t	second	s	second (or hour)	sec. (or hr.)
Force	F	weight of one kilogram	kg	weight of one pound	lb.
Power	P	kg/m/s		horsepower	hp
Speed		km/hr	k. p. h.	mi./hr.	m. p. h.
		m/s	m. p. s.	ft./sec.	f. p. s.

2. GENERAL SYMBOLS, ETC.

W, Weight, $=mg$

g, Standard acceleration of gravity $=9.80665$ m/s^2 $=32.1740$ ft./sec.^{2}

m, Mass, $=\frac{W}{g}$

ρ, Density (mass per unit volume).

Standard density of dry air, 0.12497 (kg-m^{-4} s^2) at 15° C and 760 mm $=0.002378$ (lb.-ft.$^{-4}$ sec.^{2}).

Specific weight of "standard" air, 1.2255 kg/m^3 $=0.07651$ lb./ft.^{3}

mk^2, Moment of inertia (indicate axis of the radius of gyration, k, by proper subscript).

S, Area.

S_w, Wing area, etc.

G, Gap.

b, Span.

c, Chord length.

b/c, Aspect ratio.

f, Distance from C. G. to elevator hinge.

μ, Coefficient of viscosity.

3. AERODYNAMICAL SYMBOLS

V, True air speed.

q, Dynamic (or impact) pressure $=\frac{1}{2}\rho V^2$

L, Lift, absolute coefficient $C_L=\frac{L}{qS}$

D, Drag, absolute coefficient $C_D=\frac{D}{qS}$

C, Cross-wind force, absolute coefficient $C_C=\frac{C}{qS}$

R, Resultant force. (Note that these coefficients are twice as large as the old coefficients L_C, D_C.)

i_w, Angle of setting of wings (relative to thrust line).

i_t, Angle of stabilizer setting with reference to thrust line.

γ, Dihedral angle.

$\rho\frac{Vl}{\mu}$, Reynolds Number, where l is a linear dimension.

e. g., for a model airfoil 3 in. chord, 100 mi./hr. normal pressure, 0° C: 255,000 and at 15° C., 230,000;

or for a model of 10 cm chord 40 m/s, corresponding numbers are 299,000 and 270,000.

C_p, Center of pressure coefficient (ratio of distance of C. P. from leading edge to chord length).

β, Angle of stabilizer setting with reference to lower wing, $=(i_t-i_w)$.

α, Angle of attack.

ϵ, Angle of downwash.

REPORT No. 353

AIRFOIL PRESSURE DISTRIBUTION INVESTIGATION IN THE VARIABLE DENSITY WIND TUNNEL

By EASTMAN N. JACOBS, JOHN STACK
and ROBERT M. PINKERTON

Langley Memorial Aeronautical Laboratory

NATIONAL ADVISORY COMMITTEE FOR AERONAUTICS

NAVY BUILDING, WASHINGTON, D. C.

(An independent Government establishment, created by act of Congress approved March 3, 1915, for the supervision and direction of the scientific study of the problems of flight. Its membership was increased to 15 by act approved March 2, 1929 (Public, No. 908, 70th Congress). It consists of members who are appointed by the President, all of whom serve as such without compensation.)

JOSEPH S. AMES, Ph. D., *Chairman.*
President, Johns Hopkins University, Baltimore, Md.
DAVID W. TAYLOR, D. Eng., *Vice Chairman,*
Washington, D. C.
CHARLES G. ABBOT, Sc. D.,
Secretary, Smithsonian Institution, Washington, D. C.
GEORGE K. BURGESS, Sc. D.,
Director, Bureau of Standards, Washington, D. C.
WILLIAM F. DURAND, Ph. D.,
Professor Emeritus of Mechanical Engineering, Stanford University, California.
JAMES E. FECHET, Major General, United States Army,
Chief of Air Corps, War Department, Washington, D. C.
BENJAMIN D. FOULOIS, Brigadier General, United States Army,
Chief, Matériel Division, Air Corps, Wright Field, Dayton, Ohio.
HARRY F. GUGGENHEIM, M. A.,
President, The Daniel Guggenheim Fund for the Promotion of Aeronautics, Inc., New York City.
WILLIAM P. MACCRACKEN, Jr., Ph. B.,
Chicago, Ill.
CHARLES F. MARVIN, M. E.,
Chief, United States Weather Bureau, Washington, D. C.
WILLIAM A. MOFFETT, Rear Admiral, United States Navy,
Chief, Bureau of Aeronautics, Navy Department, Washington, D. C.
S. W. STRATTON, Sc. D.,
President, Massachusetts Institute of Technology, Cambridge, Mass.
J. H. TOWERS, Commander, United States Navy,
Assistant Chief, Bureau of Aeronautics, Navy Department, Washington, D. C.
EDWARD P. WARNER, M. S.,
Editor "Aviation," New York City.
ORVILLE WRIGHT, Sc. D.,
Dayton, Ohio.

GEORGE W. LEWIS, *Director of Aeronautical Research.*
JOHN F. VICTORY, *Secretary.*
HENRY J. E. REID, *Engineer in Charge, Langley Memorial Aeronautical Laboratory, Langley Field, Va.*
JOHN J. IDE, *Technical Assistant in Europe, Paris, France.*

EXECUTIVE COMMITTEE

JOSEPH S. AMES, *Chairman.*
DAVID W. TAYLOR, *Vice Chairman.*

CHARLES G. ABBOT.
GEORGE K. BURGESS.
JAMES E. FECHET.
BENJAMIN D. FOULOIS.
WILLIAM P. MACCRACKEN, Jr.
CHARLES F. MARVIN.
WILLIAM A. MOFFETT.
S. W. STRATTON.
J. H. TOWERS.
EDWARD P. WARNER.
ORVILLE WRIGHT.

JOHN F. VICTORY, *Secretary.*

REPORT No. 353

AIRFOIL PRESSURE DISTRIBUTION INVESTIGATION IN THE VARIABLE DENSITY WIND TUNNEL

By Eastman N. Jacobs, John Stack, and Robert M. Pinkerton

SUMMARY

With a view to extending the knowledge of the aerodynamics of lifting surfaces, the distribution of pressure over one section each of six airfoils has been measured in the Variable Density Wind Tunnel of the National Advisory Committee for Aeronautics. The following airfoils were investigated: N. A. C. A. 85–J, N. A. C. A. 84–J, N. A. C. A. 84, N. A. C. A. M–6, Clark Y, and R. A. F. 30.

Pressure-distribution diagrams, as well as the integrated characteristics of the airfoils, are given for both a high and a low dynamic scale Reynolds Number or Vl/ν, for comparison with flight and other wind-tunnel tests, respectively. It is concluded that the scale effect is very important only at angles of attack near the burble. The distribution of pressure over an airfoil having a Joukowski section is compared with the theoretically derived distribution. A further study of the distribution of pressure over all of the airfoils resulted in the development of an approximate method of predicting the pressure distribution along the chord of any normal airfoil for all attitudes within the working range if the distribution at one attitude is known.

INTRODUCTION

Two distinct methods have been commonly used in investigating the aerodynamic characteristics of airfoils. One consists of measuring the mechanical forces required to support a wing in an air stream, the other consists of measuring directly the air pressures acting on the surface of the wing. Tests of the first type are spoken of as force tests, and of the second type as pressure-distribution tests. If all of the air forces were transmitted to the wing by the action of pressure alone, the results of a pressure-distribution test would be more complete than the results of a force test, because the total forces acting on the wing could be obtained by integration and, in addition, the results would show how the forces are distributed. Actually, through the action of viscosity, shear forces which are not measured in a pressure-distribution test are transmitted to the surface of the wing. Such forces account for only a small part of the total air force acting on a wing except at angles of attack near zero lift, but are sufficiently large at any angle to make the drag determination as obtained by integrating the pressures of little practical value.

Investigations of the distribution of pressures on airfoils have been conducted heretofore both in flight and in wind tunnels, but most of them have dealt chiefly with the relation of the load distribution to the strength of airplane structures. Discrepancies between flight and tunnel tests have been attributed to scale effect, but previously such tests never had been conducted at both a high and a low Reynolds Number under otherwise similar conditions in order to study any differences in the aerodynamic characteristics of airfoils which result from changing the dynamic scale. Force tests at a high and at a low scale had been conducted in the Variable Density Wind Tunnel, in order to study the scale effect on airfoils, but force tests give little information concerning any differences in the distribution of the air forces at the different dynamic scales. Pressure-distribution tests have not heretofore been made in the Variable Density Wind Tunnel because of the mechanical difficulties involved in making the measurements at the higher pressures.

The present investigation was undertaken with the object of increasing the general knowledge of the aerodynamics of lifting surfaces, but with particular reference to the distribution of pressures over airfoils at a large scale or Reynolds Number. The tests were conducted in the Variable Density Wind Tunnel of the National Advisory Committee for Aeronautics. Air pressures were measured at several points along the midsections of six airfoils. In order that the experimental and theoretical pressures could be compared, two airfoils of the Joukowski type were included, the 85–J (a symmetrical airfoil), and the 84–J. A third airfoil, the N. A. C. A. 84, is a modification of the corresponding Joukowski airfoil (Reference 6). This airfoil was included so that the effects of flattening the lower surface of a Joukowski airfoil to provide a more practical form could be studied. In addition to these airfoils, three well-known airfoils of about the same thickness were included, the R. A. F. 30 (a symmetrical airfoil), the Clark Y, and the N. A. C. A. M–6. The latter airfoil was included in order to obtain data

on the distribution of pressure over a cambered airfoil having a reflexed mean camber line to produce an approximately stationary center of pressure.

TESTS AND APPARATUS

The measurement of the pressures over the surfaces of the various airfoils treated in this investigation have been made at 3-degree intervals over a range of angle of attack from zero lift to well beyond maximum lift, and at air densities of approximately 1 and 20 atmospheres. The M–6 tests, which were performed some time after the other tests, were made at an air density of 2 atmospheres with check runs at 3 atmospheres, and observations were made at 1-degree intervals for the low angles of attack.

A description of the Variable Density Wind Tunnel, in which these tests were performed, together with a statement of the principles on which its operation is based are given in Reference 1. The description there given is, however, of the original closed throat tunnel. In its present form the tunnel differs from the original chiefly in that it is now operated as an open throat type. A diagrammatic sketch of the new tunnel is presented in Figure 1, and a photograph of the model mounting with a model in place is shown in Figure 2.

The models were of mahogany with pressure tubes inlaid. The chord was 10 inches and the span 72 inches, so that the models extended across the 60-inch jet and into the dead air space on either side. The section over which the pressures were measured was located at midstream. The locations of the orifices along this section are given in the tables of Figures 3 to 8. The M–6 model differed from the other models in that its chord was 8 inches and its span 36 inches. It was mounted on the balance wing supports since, at the time this test was performed, the original mounting had been dismantled.

Two different types of manometers were required to measure the pressures because of the large differences between the pressures encountered at the different air densities. For the 1-atmosphere or low-scale tests a multiple tube alcohol manometer, manually operated, was employed. A tube of this manometer was connected to each orifice in the wing, and one tube was connected to a static pressure orifice in the return passage of the tunnel which had been calibrated to measure the dynamic pressure. Records were taken by exposing a sheet of photostat paper placed against the tubes of the manometer. This same procedure was used for the 2 and 3 atmosphere tests, excepting that carbon tetrachloride was substituted for alcohol as the manometer liquid. The 20-atmosphere or high-scale tests required the use of an automatic recording photomanometer. A description of a similar instrument is given in Reference 2. Each cell of this manometer was connected to an orifice in the wing, and the pressures at all orifices were recorded simultaneously for a period of about 5 seconds at each angle of attack. The dynamic pressure was measured independently by means of an alcohol manometer connected to the calibrated static pressure orifice. In all cases the reference pressure for the manometers was that in the dead air space surrounding the jet.

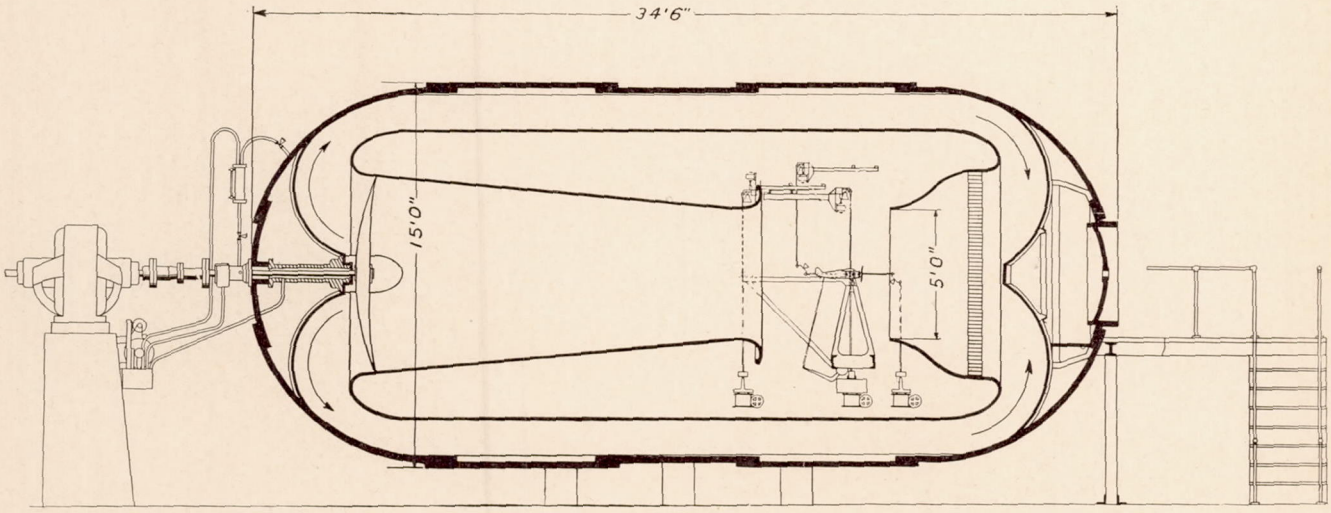

FIGURE 1.—The redesigned variable density wind tunnel

RESULTS

Values of the ratio p/q, the local pressure p at each orifice measured with respect to the pressure in the dead air space about the jet divided by the dynamic pressure q, were determined for plotting for the 1, 2, and 3 atmosphere tests by taking the ratio of the deflection in each tube to the deflection in the tube connected to the static pressure orifice and multiplying it by the orifice calibration factor. The 20-atmosphere or high-scale values of this ratio were determined in a

different manner. Here it was necessary to determine first the pressures corresponding to the deflections on the records, since each cell of the manometer had a different calibration. These pressures were then divided by the dynamic pressure which had been determined independently. The plots constructed from these values were integrated mechanically to obtain the normal force and moment coefficients, which are defined by the following expressions:

The results are presented in Figures 3 to 8. Each figure is complete in itself and presents, in addition to the pressure-distribution diagrams, a table giving the ordinates of the airfoil and the orifice locations, a sketch of the particular profile to which the figure applies, and plots of the normal force and moment coefficients. The pressure-distribution diagrams for the low and high scale have been plotted on a common chord so that they may be easily compared.

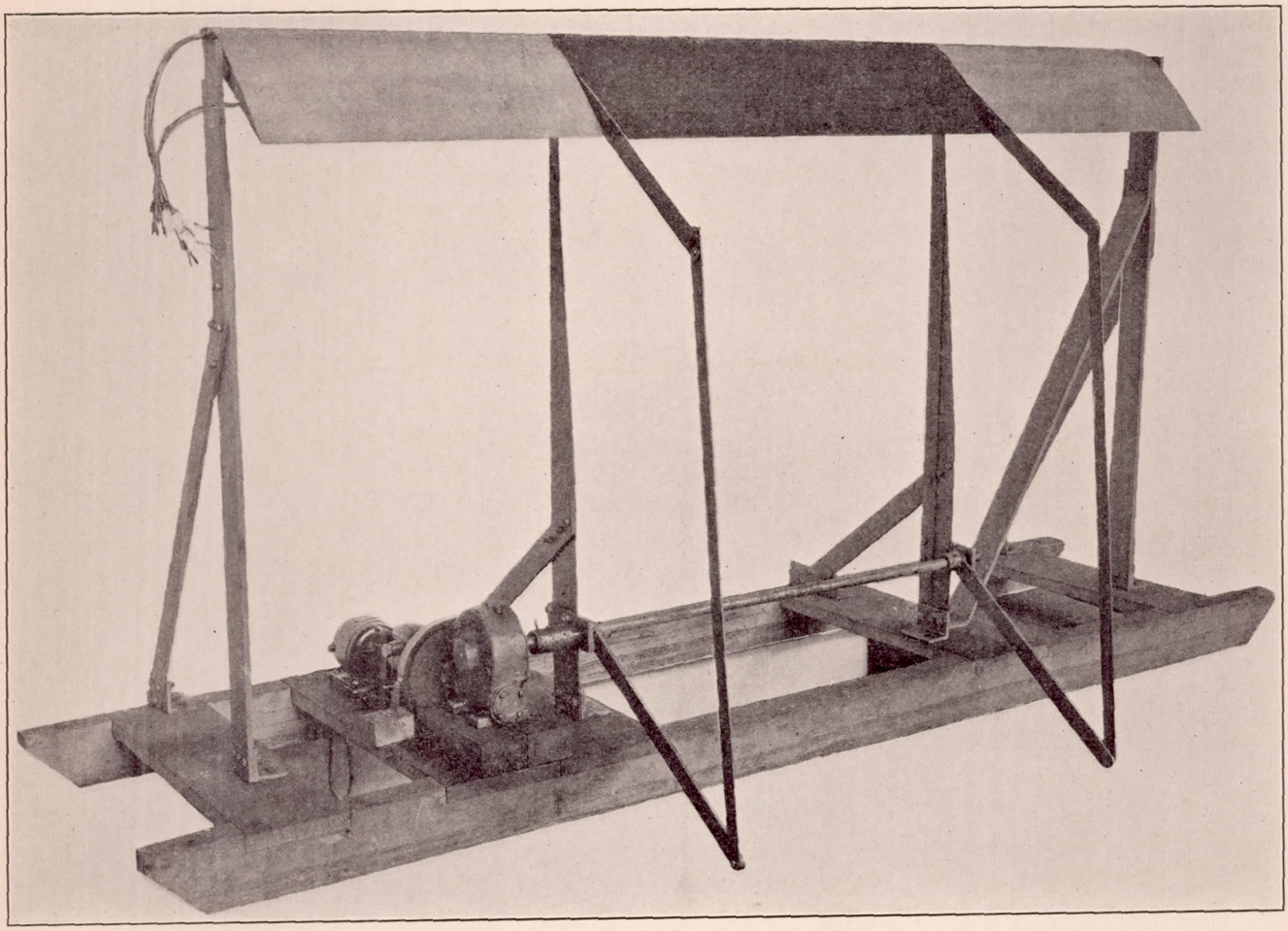

FIGURE 2.—Model airfoil mounting for pressure-distribution tests

$C_{NF}=\frac{F}{qS}$, $C_M=\frac{M}{qSc}$ where F is the resultant pressure force normal to the chord and M is the corresponding moment about a point one-quarter of the chord behind the leading edge.

The pressures over the lower surfaces of the symmetrical sections treated in this investigation, the R.A.F. 30 and N.A.C.A. 85–J, were not measured, since the conditions over the lower surfaces of these airfoils at any particular angle of attack are the same as the conditions over the upper surface at the same numerical angle of opposite sign. Thus, the distribution of pressure over the lower surface at $+3°$ was taken the same as the distribution over the upper surface at $-3°$.

In comparing the curves it must be remembered that the high-scale tests were less accurate than the low-scale tests for several reasons. The model mounting lacked sufficient rigidity to maintain accurately its angle calibration when subjected to the large forces encountered during a high-scale run. The width of the lines on the photomanometer records was of the order of that which would be produced by pressure pulsations of ± 10 per cent of the dynamic pressure, and last, the manometer cells were subject to errors in their respective calibrations. Further recent studies of the effect of temperature on the calibrations of the manometer cells have shown that errors as high as 10 per cent may have been introduced in this way. A part of the difference between the high and the low

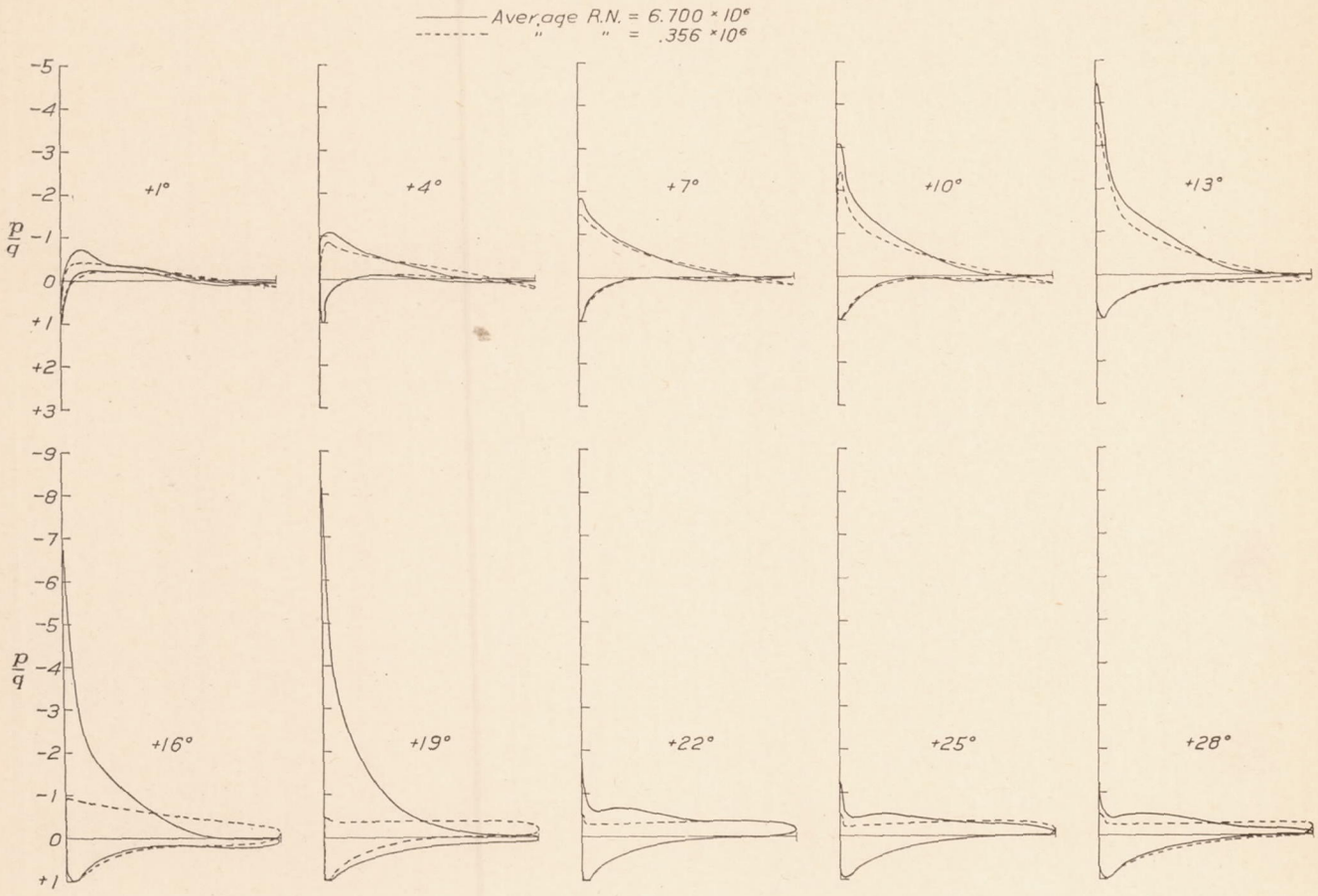

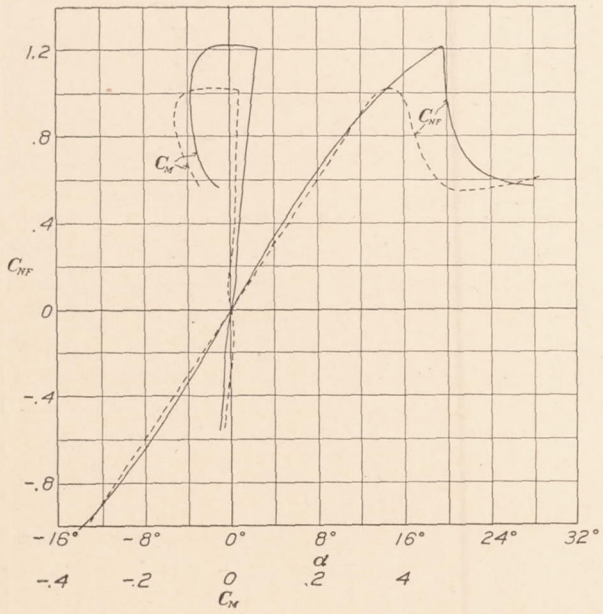

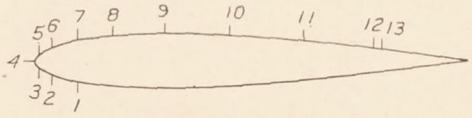

% Ch'd	Ordinates Up'r	Ordinates L'wr	Orifice No.
0	0.00	0.00	4
1			3-5
1.25	1.80	-1.80	
2.5	2.48	-2.48	
4			2-6
5	3.46	-3.46	
7.5	4.15	-4.15	
10	4.68	-4.68	1-7
15	5.44	-5.44	
18			8
20	5.94	-5.94	
30	6.32	-6.32	9
40	6.20	-6.20	
45			10
50	5.66	-5.66	
60	4.78	-4.78	
62			11
70	3.70	-3.70	
78			12
80	2.50	-2.50	13
90	1.30	-1.30	
95	0.70	-0.70	
100	0.00	0.00	

FIGURE 3.—Pressure distribution on R. A. F. 30 airfoil

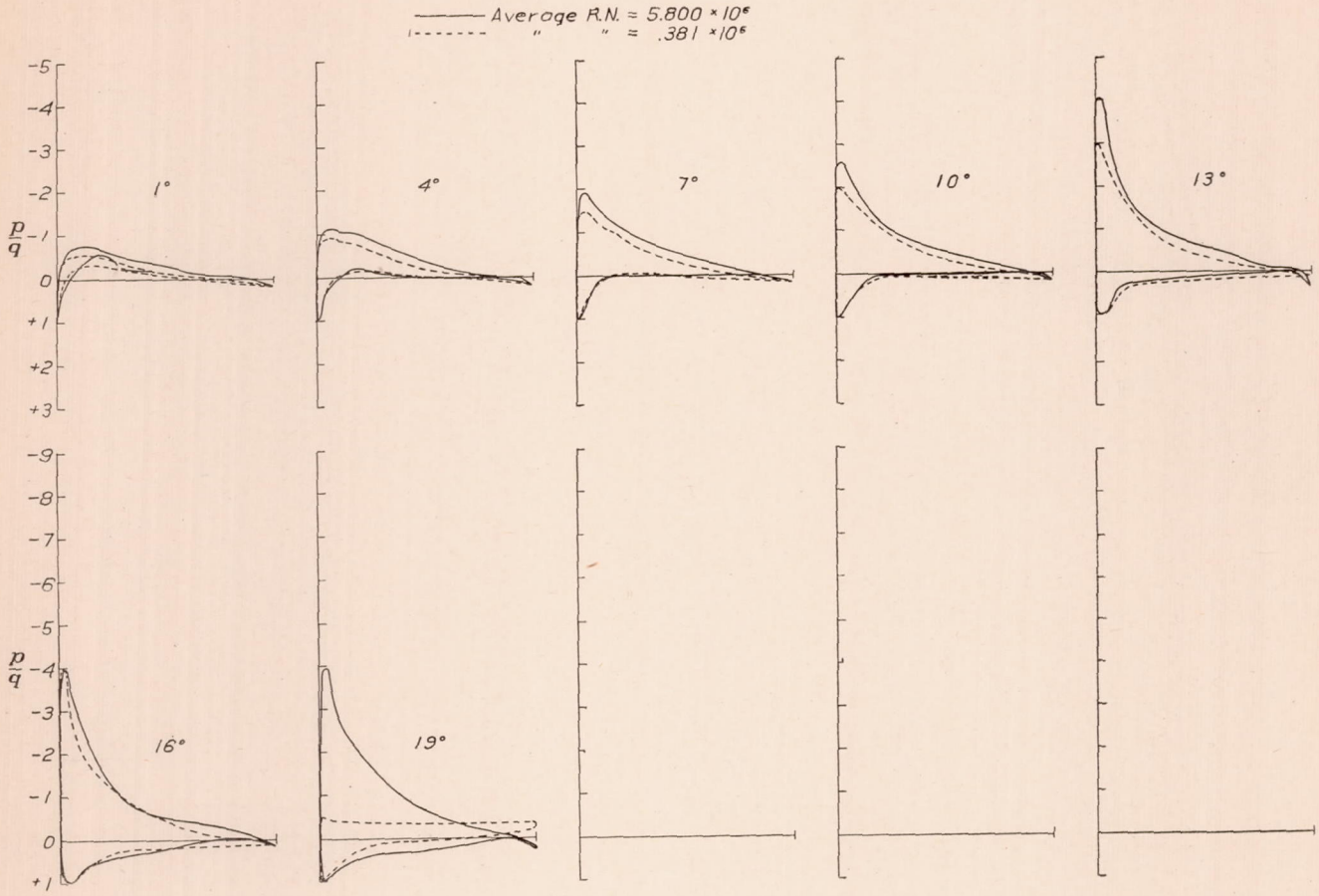

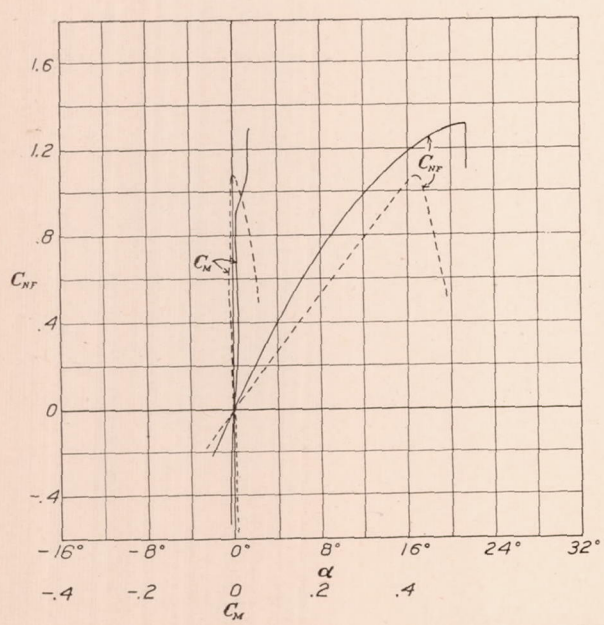

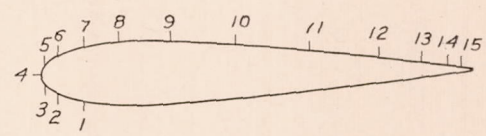

Table of ordinates and orifice locations

% Ch'd	Ordinates Up'r	Ordinates L'wr	Orifice No.	% Ch'd	Ordinates Up'r	Ordinates L'wr	Orifice No.
0	0.00	0.00	4	40	6.69	-6.69	
.50	1.53	-1.53		45			10
1			3-5	50	5.81	-5.81	
1.25	2.39	-2.39		60	4.82	-4.82	
2.50	3.38	-3.38		62			11
4			2-6	70	3.74	-3.74	
5	4.70	-4.70		78			12
7.5	5.53	-5.53		80	2.60	-2.60	
10	6.11	-6.11	1-7	88			13
15	6.90	-6.90		90	1.44	-1.44	
18			8	94			14
20	7.33	-7.33		95	0.81	-0.81	
25	7.50	-7.50		97			15
30	7.33	-7.33	9	100	0.15	-0.15	
35	7.05	-7.05					

FIGURE 4.—Pressure distribution on N. A. C. A. 85-J airfoil

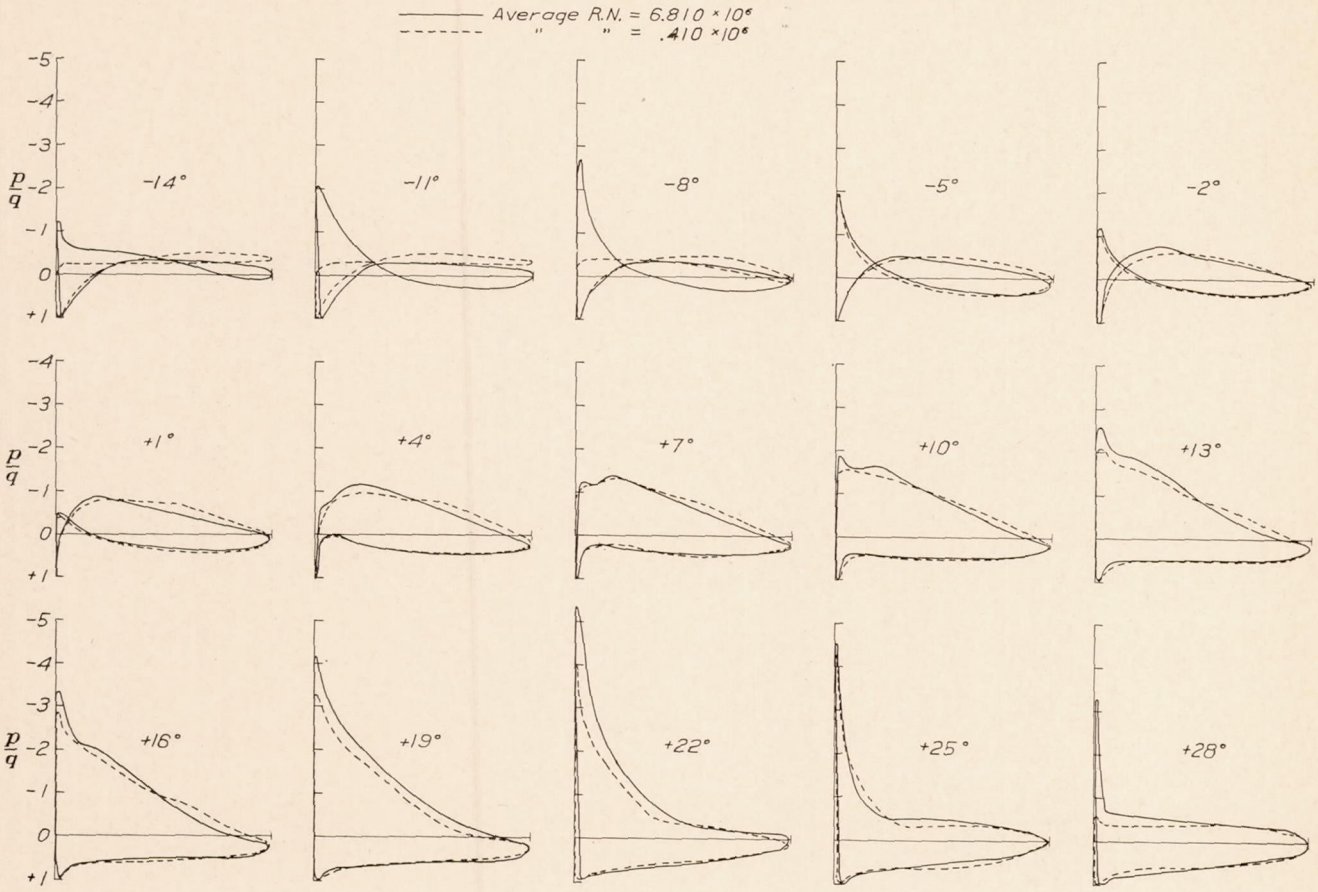

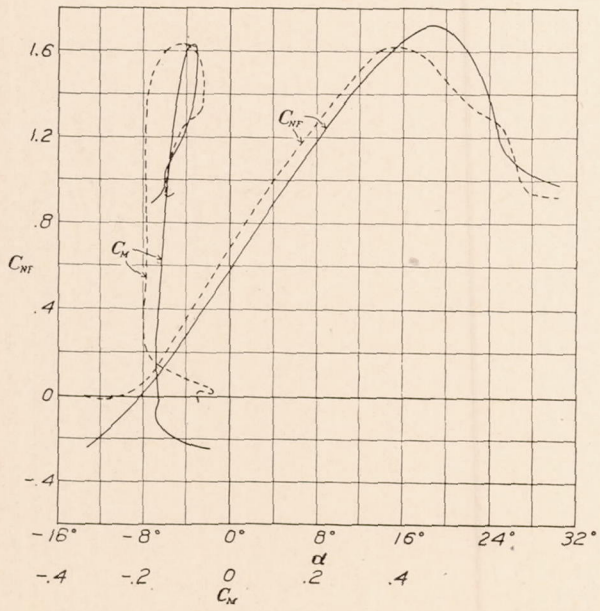

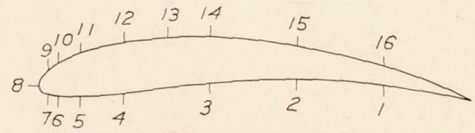

% Ch'd	Ordinates Up'r	Ordinates L'wr	Orifice No.
0	2.50	2.50	8
.50	3.90	1.55	
1.25	4.85	0.95	
2.5	6.05	0.41	7-9
5	7.78	0.10	6-10
7.5	9.03	0.02	
8.5		0.00	
10	10.00	0.04	5-11
15	11.50	0.41	
20	12.71	1.00	4-12
25	13.51	1.62	
30	14.00	2.23	13
35	14.18	2.82	
40	14.11	3.35	3-14
50	13.50	4.02	
60	12.31	4.25	2-15
70	10.32	4.02	
80	7.71	3.20	1-16
90	4.39	1.72	
95	2.41	0.84	
100	0.30	0.00	

FIGURE 5.—Pressure distribution on N. A. C. A. 84-J airfoil

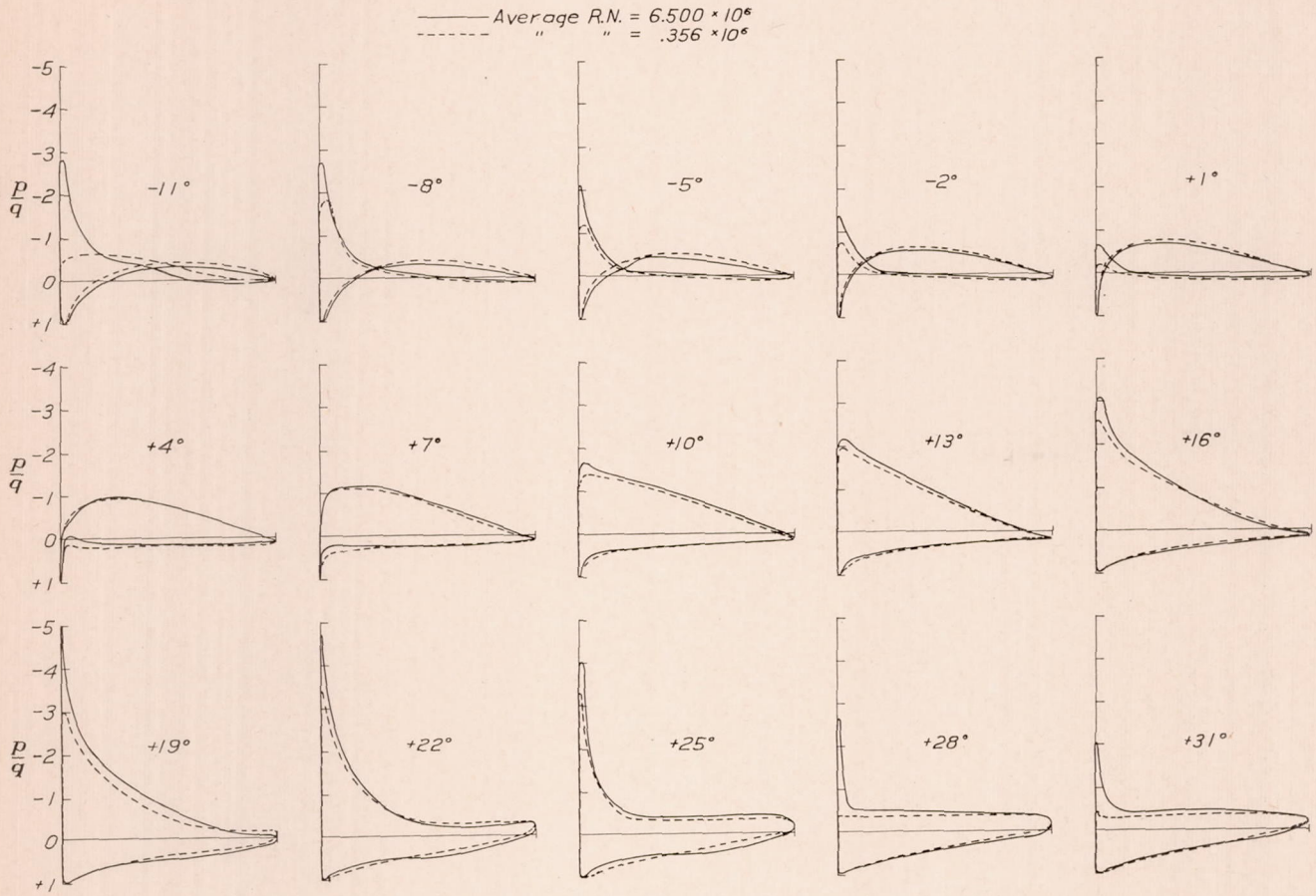

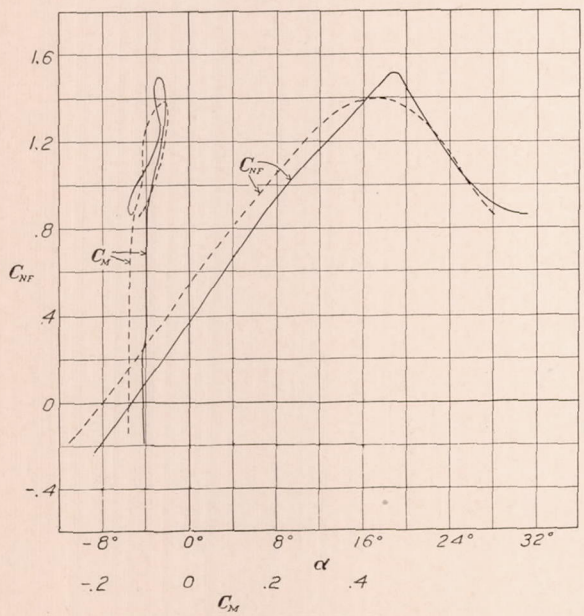

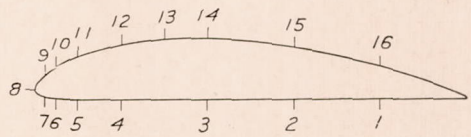

% Ch'd	Ordinates Up'r	Ordinates L'wr	Orifice No.
0	2.50	2.50	8
.50	3.90	1.55	
1.25	4.85	0.95	
2.5	6.05	0.41	7-9
5	7.78	0.10	6-10
7.5	9.03	0.02	
8.5		0.00	
10	10.00	0.00	5-11
15	11.50	0.00	
20	12.71	0.00	4-12
25	13.51	0.00	
30	14.00	0.00	13
35	14.18	0.00	
40	14.11	0.00	3-14
50	13.50	0.00	
60	12.31	0.00	2-15
70	10.32	0.00	
80	7.71	0.00	1-16
90	4.39	0.00	
95	2.41	0.00	
100	0.30	0.00	

FIGURE 6.—Pressure distribution on N. A. C. A. 84 airfoil

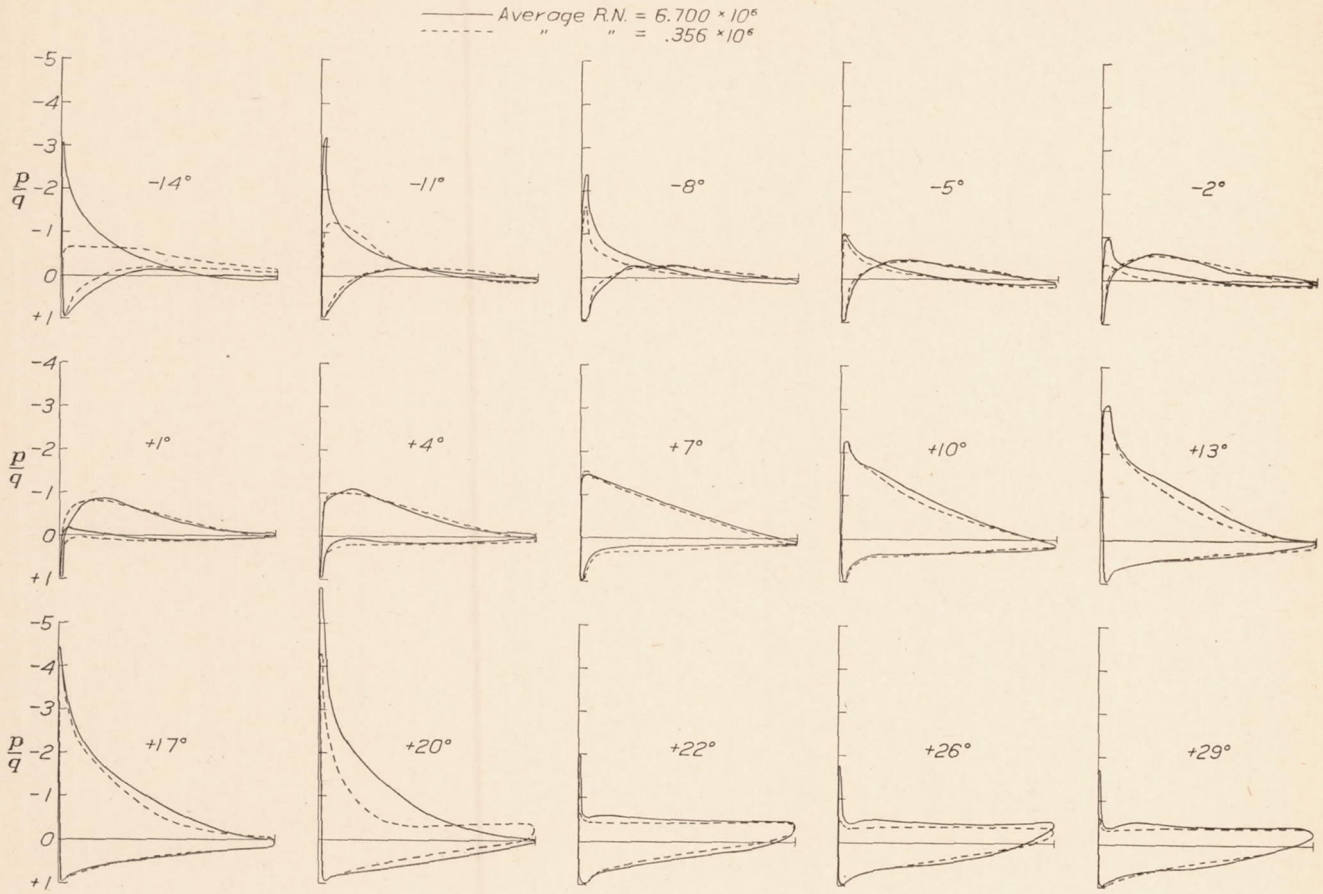

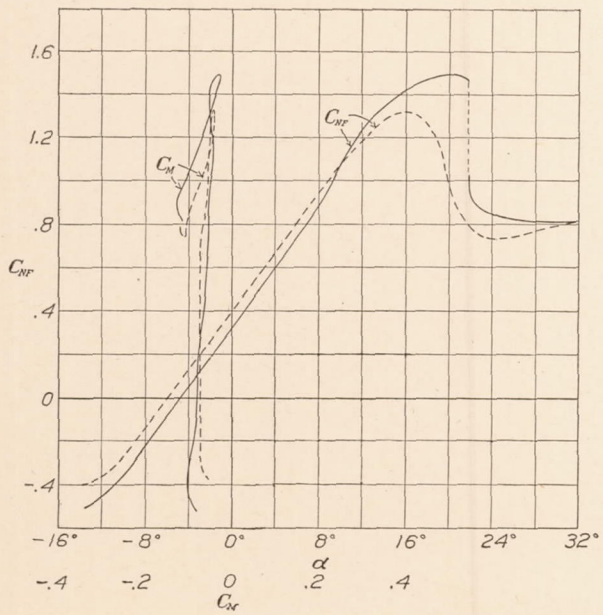

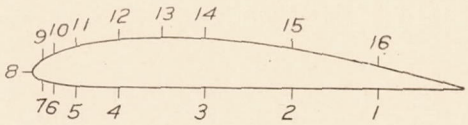

Table of ordinates and orifice locations

% Ch'd	Ordinates Up'r	Ordinates L'wr	Orifice No.
0	3.50	3.50	8
1.25	5.45	1.93	
2.5	6.50	1.47	7-9
5	7.90	0.93	6-10
7.5	8.85	0.63	
10	9.60	0.42	5-11
15	10.69	0.15	
20	11.36	0.03	4-12
30	11.70	0.00	13
40	11.40	0.00	3-14
50	10.52	0.00	
60	9.15	0.00	2-15
70	7.35	0.00	
80	5.22	0.00	1-16
90	2.80	0.00	
95	1.49	0.00	
100	0.12	0.00	

FIGURE 7.—Pressure distribution on Clark Y airfoil

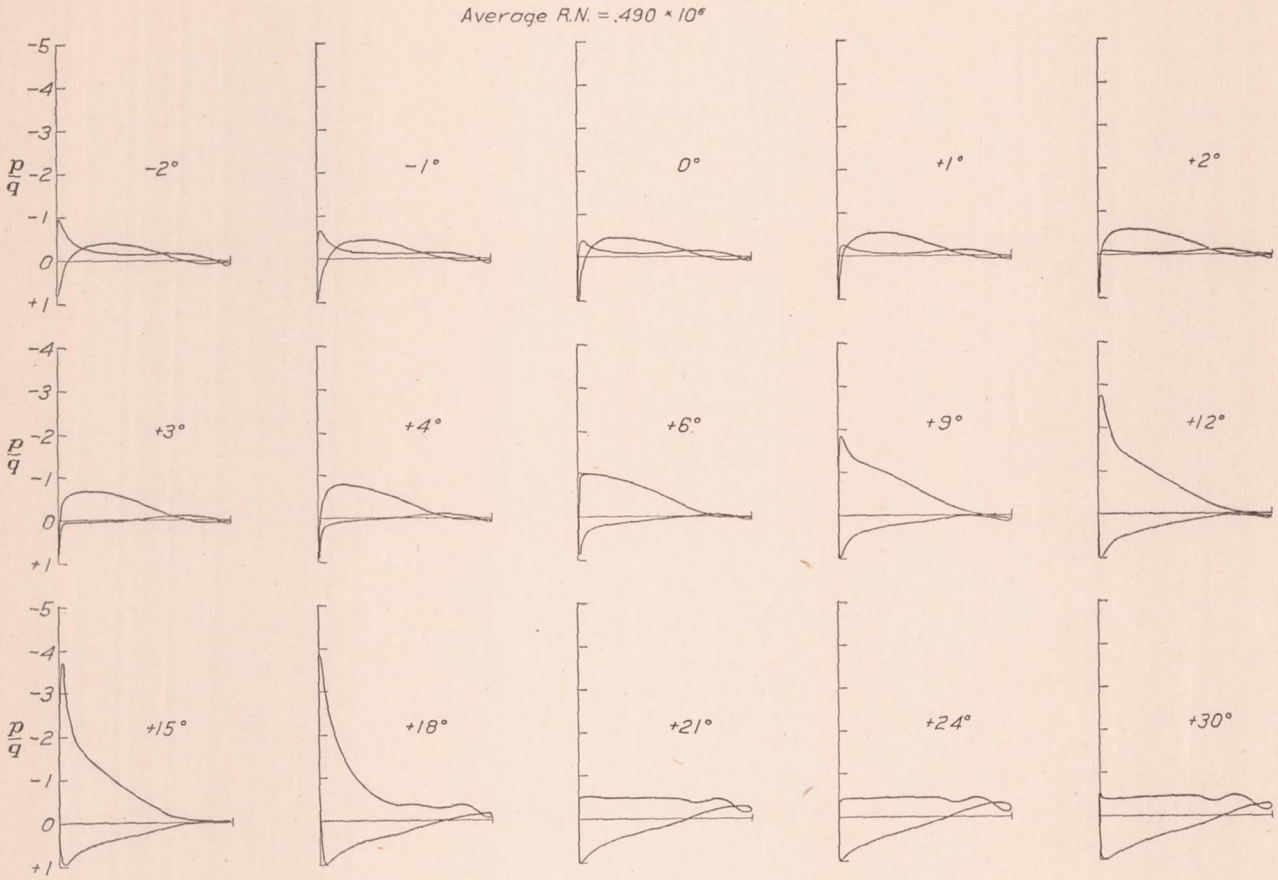

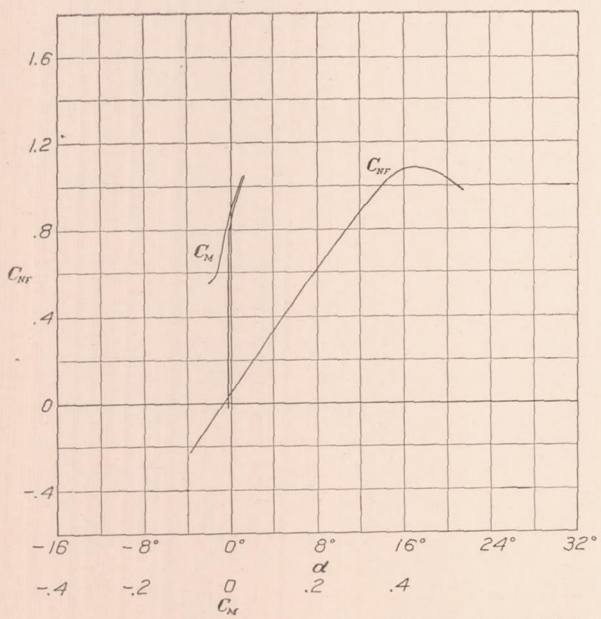

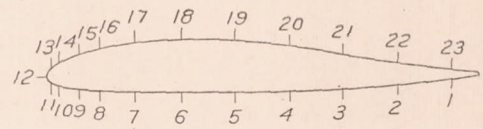

Table of ordinates and orifice locations

% Ch'd	Ordinates Up'r	Ordinates L'wr	Orifice No.	% Ch'd	Ordinates Up'r	Ordinates L'wr	Orifice No.
0	0.00	0.00	12	40.00	8.05	-3.90	
1.25	1.97	-1.76	11-13	43.75			5-19
2.50	2.81	-2.20		50.00	7.26	-3.94	
3.13			10-14	56.25			4-20
5.00	4.03	-2.73		60.00	6.03	-3.82	
7.50	4.94	-3.03		68.75			3-21
7.81			9-15	70.00	4.58	-3.48	
10.00	5.71	-3.24		80.00	3.06	-2.83	
12.50			8-16	81.25			2-22
15.00	6.82	-3.47		90.00	1.55	-1.77	
20.00	7.55	-3.62		93.75			1-23
20.63			7-17	95.00	0.88	-1.08	
30.00	8.22	-3.79		100	0.26	-0.26	
31.25			6-18				

FIGURE 8.—Pressure distribution on N. A. C. A. M-6 airfoil

scale results of these tests may, therefore, be due to inaccuracies of measurement.

DISCUSSION

Integrated Characteristics.—Airfoil characteristics obtained from pressure-distribution measurements over one section of an airfoil will differ somewhat from characteristics obtained from force tests. The greatest difference should appear in the forms of the normal force coefficient curves at maximum lift. The burble should be more critical for these tests, since the results are dependent on conditions at one section only, whereas force test results are mean values for many sections, all working at different effective angles of attack. The maximum normal force coefficient may be expected to be greater for these tests than for force tests because these measurements are made at the midsection, and the less efficient tip sections do not influence the results. The slope of the lift curve, too, will be affected by the type of test. This characteristic is dependent on down flow, and as each section along the span works at a different effective angle of attack, the force test results will represent the mean value. The results of these tests represent the conditions at the center section and, accordingly, for airfoils of the same over-all aspect ratio these tests should indicate a steeper slope than force tests. However, as the aspect ratio for these tests is problematical due to unknown end effects, differences in slope due to type of test can not be predicted. Since the moment coefficient is approximately independent of the angle of attack, and since skin friction contributes little to the pitching moment, agreement is to be expected between the values of the moment coefficient as determined from the two types of tests.

That these deductions might be verified, a comparison of the characteristics of the Clark Y airfoil as derived from these tests and from representative force tests has been made. The comparative results are shown in Figure 9. The plots shown in the figure verify the expected difference in type of burble. Predictions as to the probable behavior of the other characteristics are likewise substantiated. While it is true that the difference in Reynolds Number for the results shown in Figure 9 is rather large, very little of the differences can be ascribed to scale, since previous experiments indicate small scale effects after the Reynolds Number reaches a value approximately equivalent to that of the force tests.

Scale Effect.—The results of these experiments indicate that the effects of scale on the distribution of pressure over airfoils is important only in the neighborhood of the burble. An examination of Figures 3 to 8 indicates that the general effect of increasing the scale is to delay the burble. This effect is more pronounced for the symmetrical sections (figs. 3 and 4) than for the nonsymmetrical sections. The ultimate result is an increase in the maximum normal force coefficient and an increase in the useful angular range of the airfoils. This increase in the angular range of angle of attack may lead to peak pressures near the nose of airfoils in flight, which are higher than the corresponding pressures indicated by low-scale tunnel tests. For example, the maximum negative pressure recorded near the nose of the R. A. F. 30 airfoil at a scale corresponding to that used in most wind tunnels was approximately three and one-half times the dynamic pressure, whereas at a scale corresponding more nearly to that of flight, maximum negative pressures of over eight times the dynamic pressure were recorded. Over the normal working range of airfoils, however, where the drag is low, the results of pressure distribution tests

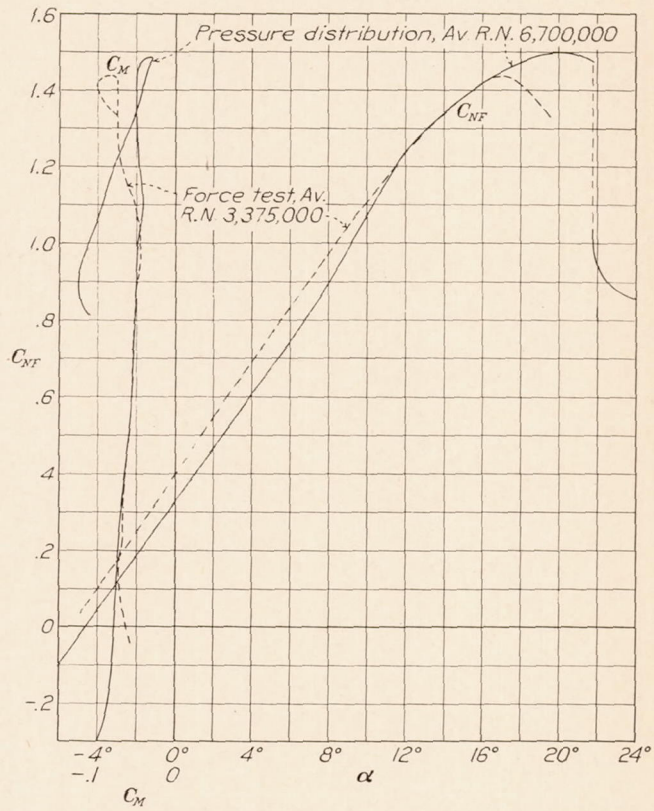

FIGURE 9.—Normal force and moment coefficients versus angle of attack

on models are not subject to important scale effect corrections.

Comparison with Theoretical Pressure Distribution.—The validity of the theoretical methods for determining the pressure distribution over airfoils is doubtful because of certain simplifying assumptions which must be made so that the mathematical relationships of the analysis will not become unmanageable. The reliability of the analysis can be determined only by a comparison with actual results, and accordingly, the pressure distribution has been measured over an airfoil for which the theoretical distribution is known, and a comparison has been effected as part of this investigation. The high-scale results, because of

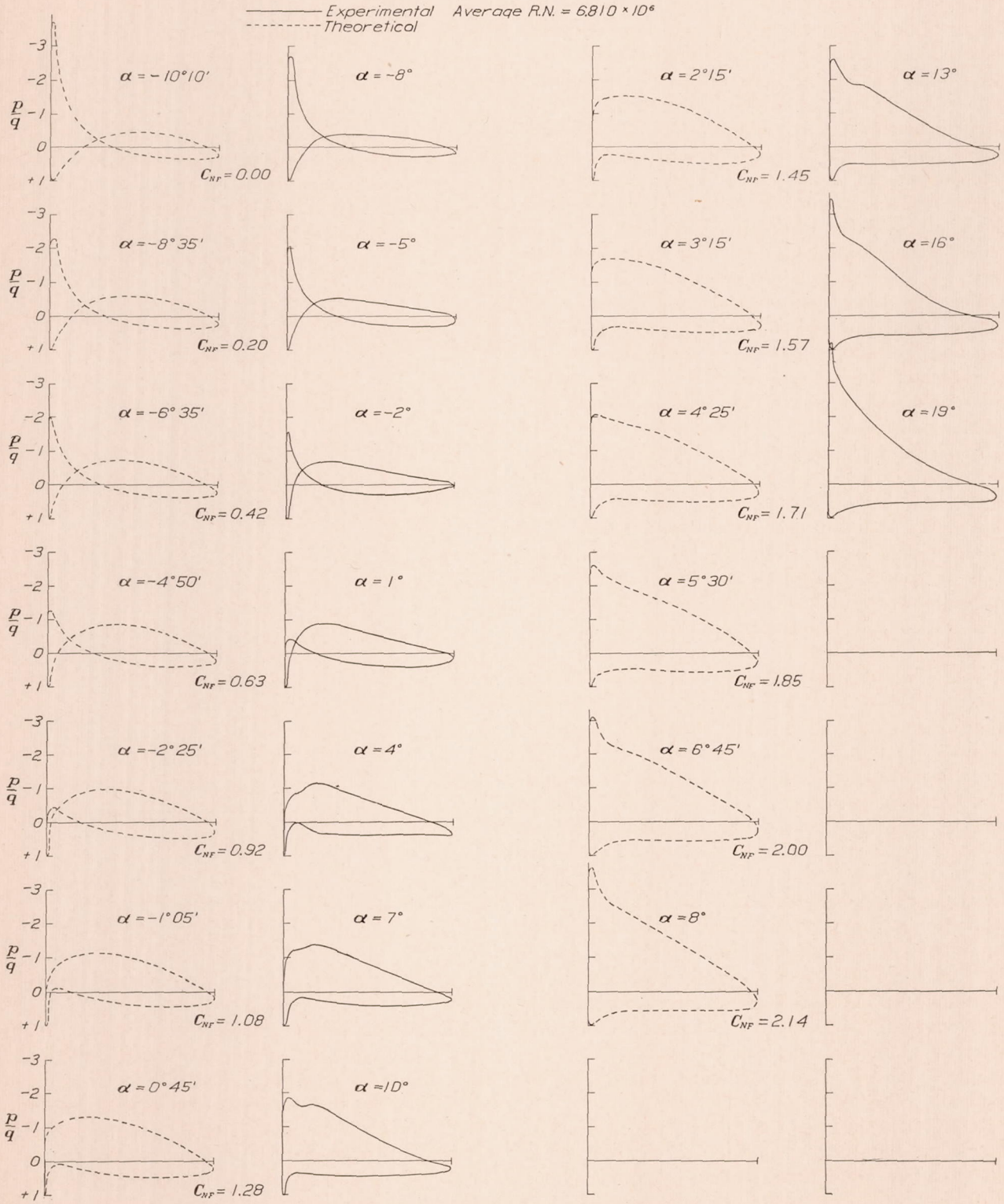

FIGURE 10.—Pressure distribution on N. A. C. A. 84-J airfoil

the relatively smaller effect of viscosity, might be expected to agree more closely than the low-scale results with the theoretical pressure distribution.

The N. A. C. A. 84–J, a Joukowski airfoil, was chosen for this investigation because the theoretical distribution of pressure could readily be determined. The theoretical method employed (Reference 3) requires, in order to define the airfoil, the establishment of the values of the mean camber (f/l) and thickness (δ/l) which are, for this particular airfoil, 0.15 and 0.05 respectively.

The graphical method of Trefftz, given in the above reference, was used to obtain the ratio $\frac{v}{V}$, the local velocity v at a point on the surface of the airfoil divided by the free stream velocity V. The corresponding value of the ratio p/q was obtained by applying Bernoulli's theorem in the form:

$$p/q = 1 - \left(\frac{v}{V}\right)^2.$$

The theoretical pressure-distribution diagrams are compared with the measured results in Figure 10. The comparison is made at equal values of the normal force coefficient and the dissimilarity between diagram forms is self-evident. This might have been expected, since it is well known that the theory of airfoils in a nonviscous fluid predicts a lift curve slope which is greater than the experimentally predicted slope of an infinite wing. A study of the figure will give interesting results. For example, considering the theoretical diagram having $C_{NF}=1.28$, it is at once noted that it compares more favorably with an experimental diagram having a lower angle of attack apparently in the region of 3° to 6°. This indicates that the diagrams might be better compared on a basis of equal angles of attack, the angle for the experimental results being the effective angle of attack, i. e., "the angle of attack at which an airfoil of infinite span (in air, a viscous fluid) would give the same lift coefficient as the airfoil of finite span under consideration" (Reference 7). This comparison is not possible, in this instance, since the down flow produced by the wing in the tunnel is not known. However, it should be noted that for diagrams at the same angle of attack the theoretical diagram will have the greater area. This means, then, that the full theoretical value of the circulation about an airfoil at any given angle of attack is not actually attained.

Differences between the theoretical pressure distribution and results of high and low scale tests can be observed by referring back to Figure 5. It is obvious that the low scale results agree with the theory equally as well as the high scale results while the flow is steady. The high scale results do, however, show a slightly greater range of similarity to the theoretical since the effect of increased scale is to increase the range of steady flow.

Prediction of the Force Distribution along the Chord.—The difficulties involved in an analytical determination of the forces over airfoils having empirical profiles are so great that experimental methods only have been used. Inasmuch as some of our most common profiles are empirical, it would seem appropriate that the problem of analytically determining the air-force distribution on such airfoils be given some attention. A study of this question in connection with these tests has resulted in the development of an approximate method for determining the force distribution over any airfoil provided the distribution at zero lift is known.

The theory of the thin wing, as developed by Munk (Reference 5), separates the air forces acting on any wing into two parts. The first of these two are forces which produce the lift and no moment. They are so distributed along the chord that their resultant acts at a point one quarter of the chord aft of the leading edge regardless of the airfoil shape. The second part consists of forces which produce a couple but no lift. The distribution of these forces is such that the value of the couple remains constant for all angles, and is dependent only on the shape of the mean camber line of the airfoil.

If we assume that the distribution of the air forces which produces the lift is independent of the airfoil shape, basing this assumption on the theory that their resultant point of application is independent of the airfoil shape, we can determine this part of the air force distribution for any desired value of the force coefficient by calculating the distribution over a theoretically derived symmetrical section. In the same manner, if we assume that the distribution of the air forces which produce the moment is independent of the lift, basing this assumption on the theory that the value of the moment is independent of the lift, we can determine this part of the air force distribution by measuring the pressure distribution at zero lift. The force distribution on the airfoil will then be obtained by adding the lift and moment distributions.

When the force distribution on the airfoil at zero lift is known, to find the distribution corresponding to any value of the force coefficient, it is only necessary to add the force distribution which will produce the desired force. This distribution has been calculated after the method of Reference 4 for a symmetrical Joukowski section of 10 per cent thickness. The normal force distribution diagram for a normal force coefficient of 1.0 is reproduced in Figure 11. The ordinates, P/q, of this diagram represent the ratio of the differential pressure P, between the upper and lower surfaces, to the dynamic pressure q. They are practically proportional to the force coefficient and, therefore, only one diagram has been calculated theoretically. The diagrams for other values of the normal force coefficient are obtained by multiplying the ordinates

of the diagram in Figure 11 by the normal force coefficient. To check the validity of this assumption the distribution of pressure at zero lift as determined from experiment has been deducted from the experimental distributions for each airfoil, and the ordinates of the resulting diagrams have been scaled to give a normal force coefficient of 1. A mean curve has been

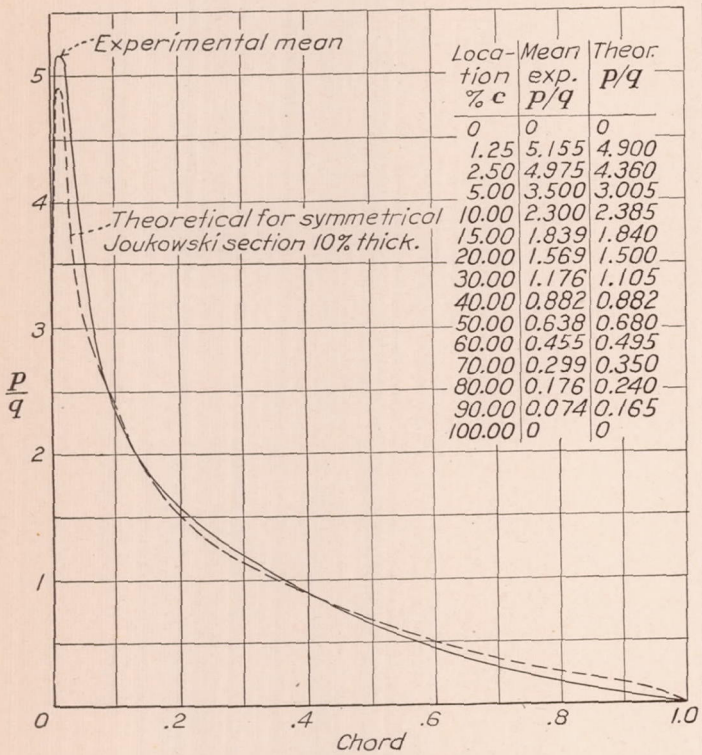

FIGURE 11.—Lift force distribution for $C_{NF_-}=1$

drawn for these diagrams and is presented in Figure 11 for comparison with the theoretical.

The force distributions over the nonsymmetrical profiles treated in this investigation have been calculated, and are compared with the experimental values in Figure 12. The major differences occur at the high force coefficients, but disagreement could be expected in this region since the assumptions of the theory no longer hold true. Closest agreement between the calculated and experimental force distributions is shown by the M-6 airfoil, probably because the experimental pressure distributions over this airfoil were measured with greater accuracy.

CONCLUSIONS

1. The accuracy of these experiments is insufficient to justify conclusions regarding small differences in the distribution of pressure over airfoils as a result of scale effect. It may be concluded that the scale effect is very important only at angles of attack near the burble.

2. The present investigation would indicate that the method of predicting the force distribution over airfoils as outlined in this report is sufficiently accurate for practical purposes.

LANGLEY MEMORIAL AERONAUTICAL LABORATORY,
NATIONAL ADVISORY COMMITTEE FOR AERONAUTICS,
LANGLEY FIELD, VA., *January 14, 1930.*

REFERENCES

1. Munk, Max M., and Miller, E. W.: The Variable Density Wind Tunnel of the National Advisory Committee for Aeronautics. N. A. C. A. Technical Report No. 227, 1927.
2. Norton, F. H., and Brown, W. G.: The Pressure Distribution Over the Horizontal Surfaces of an Airplane–III. N. A. C. A. Technical Report No. 148, 1922.
3. Blumenthal, Otto, and Trefftz, E.: Pressure Distribution on Joukowski Wings and Graphic Construction of Joukowski Wings. N. A. C. A. Technical Memorandum No. 336, 1925.
4. Perring, W. G. A.: The Theoretical Pressure Distribution Around Joukowski Aerofoils. British A. R. C., R. & M. No. 1106, 1927.
5. Munk, Max M.: Elements of the Wing Section Theory and of the Wing Theory. N. A. C. A. Technical Report No. 191, 1927.
6. Knight, M., and Bamber, M. J.: Preliminary Report on the Flat-Top Lift Curve as a Factor in Control at Low Speed. N. A. C. A. Technical Note No. 297, 1928.
7. Higgins, George J.: The Prediction of Airfoil Characteristics. N. A. C. A. Technical Report No. 312, 1929.

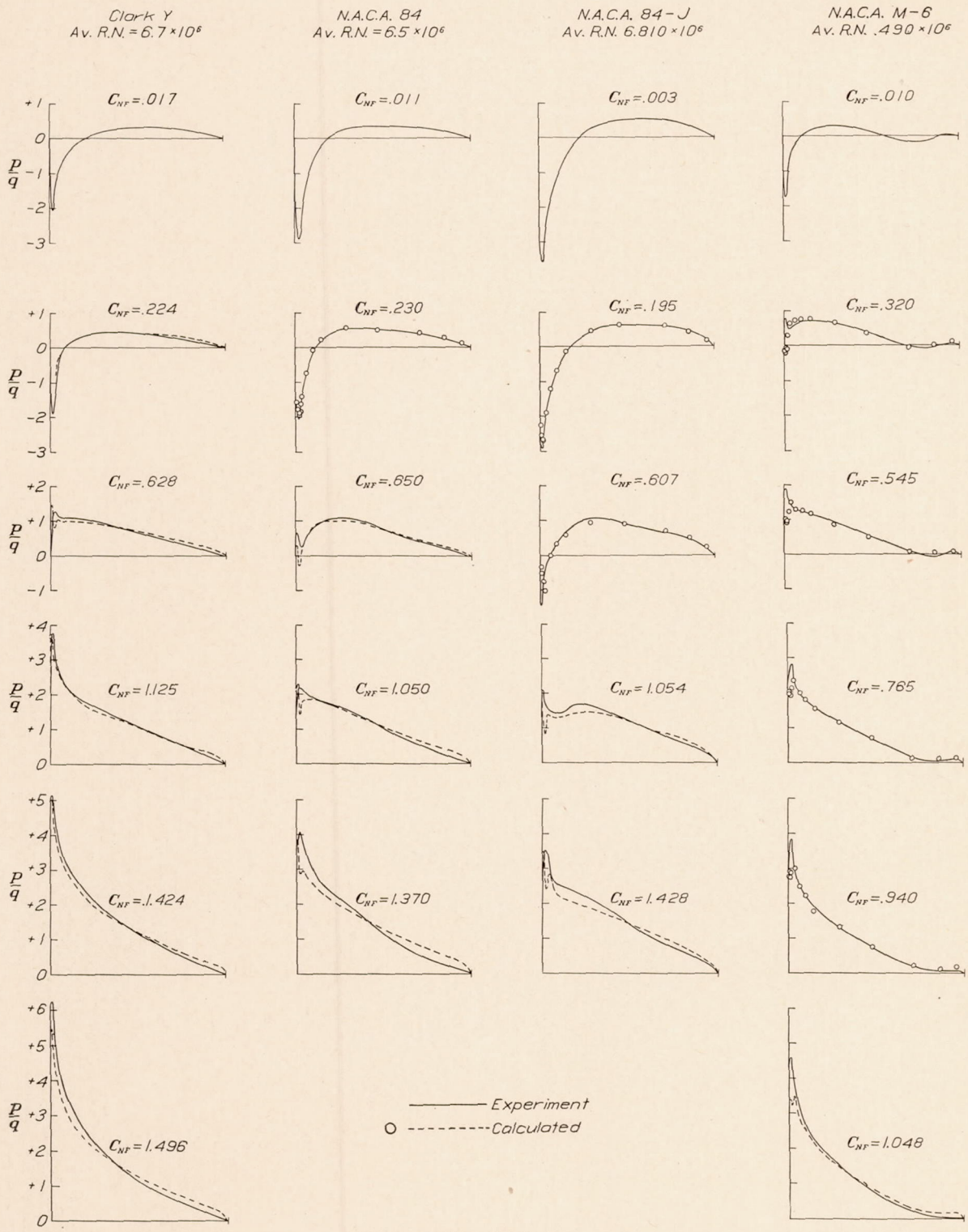

FIGURE 12.—Force distribution

U. S. GOVERNMENT PRINTING OFFICE: 1930

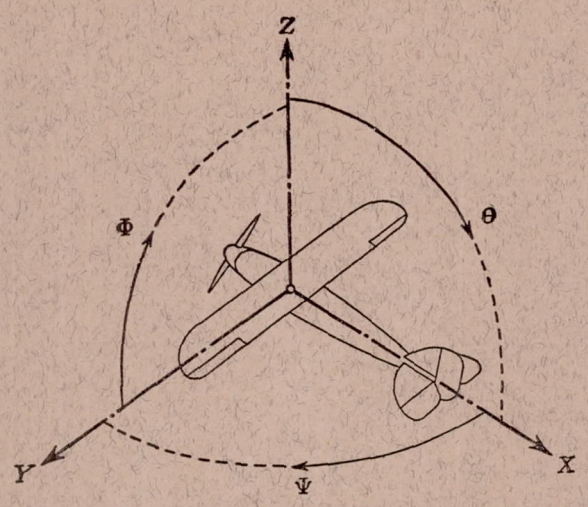

Positive directions of axes and angles (forces and moments) are shown by arrows

Axis		Force (parallel to axis) symbol	Moment about axis			Angle		Velocities	
Designation	Symbol		Designation	Symbol	Positive direction	Designation	Symbol	Linear (component along axis)	Angular
Longitudinal	X	X	rolling	L	$Y \longrightarrow Z$	roll	Φ	u	p
Lateral	Y	Y	pitching	M	$Z \longrightarrow X$	pitch	Θ	v	q
Normal	Z	Z	yawing	N	$X \longrightarrow Y$	yaw	Ψ	w	r

Absolute coefficients of moment

$$C_L = \frac{L}{qbS} \qquad C_M = \frac{M}{qcS} \qquad C_N = \frac{N}{qfS}$$

Angle of set of control surface (relative to neutral position), δ. (Indicate surface by proper subscript.)

4. PROPELLER SYMBOLS

D, Diameter.
p_e, Effective pitch.
p_g, Mean geometric pitch.
p_s, Standard pitch.
p_v, Zero thrust.
p_a, Zero torque.
p/D, Pitch ratio.
V', Inflow velocity.
V_s, Slip stream velocity.

T, Thrust.
Q, Torque.
P, Power.
(If "coefficients" are introduced all units used must be consistent.)
η, Efficiency $= T\ V/P$.
n, Revolutions per sec., r. p. s.
N, Revolutions per minute, r. p. m.
Φ, Effective helix angle $= \tan^{-1}\left(\frac{V}{2\pi rn}\right)$

5. NUMERICAL RELATIONS

1 hp = 76.04 kg/m/s = 550 lb./ft./sec.
1 kg/m/s = 0.01315 hp
1 mi./hr. = 0.44704 m/s
1 m/s = 2.23693 mi./hr.

1 lb. = 0.4535924277 kg
1 kg = 2.2046224 lb.
1 mi. = 1609.35 m = 5280 ft.
1 m = 3.2808333 ft.